Decorin Suppresses Prostate Tumor Growth through Inhibition of Epidermal Growth Factor and Androgen Receptor Pathways[1]

Yunping Hu*, Haiguo Sun*, Rick T. Owens[†],
Jiansheng Wu[‡], Yong Q. Chen[‡],
Isabelle M. Berquin[‡], Donna Perry[†],
Joseph T. O'Flaherty[§] and Iris J. Edwards*

*Department of Pathology, Wake Forest University
School of Medicine, Winston-Salem, NC 27157, USA;
[†]LifeCell Corporation, One Millennium, Branchburg, NJ
08876, USA; [‡]Department of Cancer Biology, Wake Forest
University School of Medicine, Winston-Salem, NC 27157,
USA; [§]Department of Medicine, Wake Forest University
School of Medicine, Winston-Salem, NC 27157, USA

Abstract

Epidermal growth factor receptor (EGFR) and androgen receptor (AR) pathways play pivotal roles in prostate cancer progression. Therefore, agents with dual-targeting ability may have important therapeutic potential. Decorin, a proteoglycan present in the tumor microenvironment, is known to regulate matrix assembly, growth factor binding, and receptor tyrosine kinase activity. Here, we show that in prostate-specific Pten$^{P-/-}$ mice, a genetically defined, immune-competent mouse model of prostate cancer, systemic delivery of decorin inhibits tumor progression by targeting cell proliferation and survival pathways. Moreover, in human prostate cancer cells, we show that decorin specifically inhibits EGFR and AR phosphorylation and cross talk between these pathways. This prevents AR nuclear translocation and inhibits the production of prostate specific antigen. Further, the phosphatidylinositol-3 kinase (PI3K)/Akt cell survival pathway is suppressed leading to tumor cell apoptosis. Those findings highlight the effectiveness of decorin in the presence of a powerful genetic cancer risk and implicate decorin as a potential new agent for prostate cancer therapy by targeting EGFR/AR-PI3K-Akt pathways.

Neoplasia (2009) 11, 1042–1053

Introduction

Prostate cancer is the most common form of cancer and the second leading cause of cancer-related death among men in the United States. Its development in humans proceeds through multiple defined steps: prostatic intraepithelial neoplasia, prostate cancer *in situ*, invasive, and hormone-dependent or -independent metastatic cancer. Despite the initial efficacy of androgen deprivation therapy, tumor cells eventually relapse into hormone-refractory prostate cancer [1]. The therapeutically critical switch of prostate cancer to androgen independence and distant metastasis requires an interactive microenvironment to facilitate survival and proliferation of malignant cells [2]. Therefore, identifying signaling events emanating from the microenvironment may lead to novel therapeutic targets for prostate cancer.

Decorin is a small leucine-rich proteoglycan secreted mainly by cells of mesenchymal origin. It is an important regulator of collagen fibrillogenesis and extracellular matrix assembly, as well as cell attachment and migration [3], and is involved in physiological processes including inflammatory responses [4] and wound healing [5]. Its presence in the

tumor microenvironment is proposed to reflect an attempt by the stroma to wall off the tumor [6,7]. Importantly, decorin has been shown to exert powerful growth-inhibitory properties through effects on tyrosine kinase signaling [8,9]. It is markedly upregulated during quiescence in fibroblasts and vascular smooth muscle cells [10,11], but its expression is suppressed or totally abrogated in a variety of tumors of epithelial origin such as colon, pancreas, and breast [12]. A number of human cancer cell

lines do not express decorin [13,14], and forced expression of decorin in cancer cell lines *in vitro* caused a severe cytostatic effect. Known mechanisms for cell growth inhibition by decorin include up-regulation of the cell cycle inhibitor p21 [14–16] and p27 [17], down-regulation of epidermal growth factor receptor (EGFR) [9,18], blockade of the transforming growth factor β signaling pathway [19,20], and suppression of tumor cell production of angiogenic factors such as vascular endothelial growth factor [21,22].

In mice, targeted disruption of both *decorin* and *P53* genes resulted in the acceleration of malignant lymphomas [23]. More recently, a report showed that 30% of decorin-deficient mice developed spontaneous intestinal tumors [24]. Furthermore, recombinant human decorin has been shown to inhibit the growth of tumor xenografts including those derived from breast, colon, and squamous carcinoma [25], lung and liver carcinoma [26], and gliomas [27]. However, the effects of systemically delivered decorin have not previously been studied in an immune-competent animal model with a defined genetic cancer risk or in any studies in prostate cancer.

Because decorin was shown to be expressed in high-grade human prostatic intraepithelial neoplasia but not in prostate cancer [28], we hypothesized that decorin may function in a cancer-inhibitory role in the prostate. To demonstrate such a role, we used prostate-specific Pten (phosphatase and tensin homolog deleted on chromosome 10) knockout mice, an immune-competent, orthotopic model of prostate cancer, and studied the effects of exogenous decorin on tumor growth. In this model and in cultured human prostate cancer cell lines, decorin inhibited growth and induced apoptosis. It did so by the inhibition of the EGFR, androgen receptor (AR), and phosphatidylinositol-3 kinase (PI3K)/Akt signal pathways.

Materials and Methods

Cell Lines and Reagents

DU145, LNCaP, and PC3 cells were purchased from the American Type Culture Collection (Manassas, VA) and maintained in Eagle's minimum essential medium with Earle's salts containing 10% fetal bovine serum (FBS), 1.5 g/L NaHCO$_3$, and 1% L-glutamine (DU145 cells); RPMI-1640 medium plus 10% FBS, 1.5 g/L sodium bicarbonate, 4.5 g/L glucose, 10 mM HEPES, and 110 mg/L sodium pyruvate (LNCaP cells); or advanced Dulbecco's modified Eagle medium (DMEM) containing 1% FBS and 1% L-glutamine (PC3 cells). CellTiter 96 AQueous One Solution Cell Proliferation Assay and Caspase–Glo 3/7 Assay were purchased from Promega (Madison, WI). AG1478 was purchased from Invitrogen Corporation (Carlsbad, CA), and bicalutamide was from Toronto Research Chemicals, Inc. (North York, Ontario, Canada). [^{3}H]-Thymidine was purchased from PerkinElmer Life and Analytical Sciences (Boston, MA). Advanced DMEM, Eagle's minimum essential medium with Earle's salts, and FBS were purchased from Invitrogen, and HyQ RPMI 1640 medium was purchased from Hyclone (Logan, UT). Bovine anti-Akt, anti–phospho-Akt (Ser 473), anti-PI3 kinase 110α, anti-AR, anti-EGFR, anti–phospho-EGFR (Tyr 1068), anti-PARP, anti–cyclic adenosine monophosphate response element binding protein, and anti–glyceraldehyde-3-phosphate dehydrogenase were purchased from Cell Signaling Technology (Danvers, MA). Anti-AR (N-20) was purchased from Santa Cruz Biotechnology (Santa Cruz, CA). Anti-PSA and anti–phospho-AR (Ser 213/210) were purchased from Imgenex (Fremont, CA). Anti–β-actin antibody, wortmannin, and dihydrotestosterone (DHT) was purchased from Sigma-Aldrich Company Ltd.

(Allentown, PA). Horseradish peroxidase–conjugated secondary antibodies against mouse and rabbit were purchased from Imgenex and Cell Signaling Technology, respectively.

Expression and Purification of Decorin and Biglycan Core Protein

Recombinant decorin and biglycan were expressed as a polyhistidine fusion protein in 293-EBNA cells using a CelliGen Plus Bioreactor (New Brunswick Scientific, Edison, NJ) as described previously [29,30]. In brief, cells were grown in DMEM containing 5% FBS to achieve the desired cell number. Media were then changed to serum-free conditioned media collected every 48 hours. Initial purification of decorin and biglycan proteoglycan and core protein was performed by passing 293 conditioned media over a nickel-chelating column followed by elution with a gradient of 0 to 250 mM imidazole in 20 mM Tris-HCl, 500 mM NaCl, 0.2% 3-[(3-cholamidopropyl)dimethylamino]-1-propanesulfonate, pH 8.0. Core protein was then separated from proteoglycan using anion-exchange chromatography on Q-Sepharose (Amersham Biosciences, Uppsala, Sweden).

Prostate-Specific Pten Knockout Mice

As previously described [31–33], prostate-specific Pten knockout mice were generated by crossing Pten loxP/loxP mice with mice of the ARR2Probasin-Cre transgenic line PB-cre4, wherein the Cre recombinase is under the control of a modified rat prostate-specific probasin promoter. B6.129S4-Gt (ROSA) 26Sor^{tm1Sor}/J mice, which have a floxed *lacZ* gene targeted to the ROSA26 locus, whose expression depends on Cre activity, were purchased from the Jackson Laboratory (Bar Harbor, ME). For simplicity, Pten$^{loxP/loxP}$PB-cre4$^{-/-}$ and Pten^{loxP}/$^+$PB-cre4$^{-/-}$ are referred to as Pten$^{P+/+}$ and Pten$^{loxP/loxP}$ PB-cre4$^{T/-}$ as Pten$^{P-/-}$. After weaning, Pten$^{P-/-}$ mice were injected intraperitoneally on alternate days with decorin (10 mg/kg body weight), biglycan (10 mg/kg body weight), or saline. This concentration was based on that shown to inhibit the growth of squamous cell carcinoma xenografts [29]. After the 12-week treatment, individual prostate lobes (anterior, dorsolateral, and ventral) were dissected and separated under a stereomicroscope. For later use for protein and RNA preparation, tissues were snap-frozen in liquid nitrogen and stored at –70°C until analysis. Prostates used for immunohistochemistry analysis were fixed in 10% buffered formalin. Histopathologic evaluation of mouse prostate tissues was performed by board-certified veterinary pathologists with a double-blind method. The protocol was approved by our institutional animal care and use committee.

Immunohistochemical Analysis

Mouse prostate tumor tissues were fixed in buffered formalin and embedded in paraffin. For all immunohistochemical staining (Ki-67 and caspase 3), at least two sections of each prostate lobe were assessed. Pretreated sections were incubated with rabbit monoclonal anti–Ki-67 (Lab Vision/NeoMarkers, Fremont, CA) or rabbit polyclonal anti–cleaved caspase 3 (Cell Signaling Technology) followed by a biotinylated antirabbit secondary antibody and streptavidin alkaline phosphatase (Super Sensitive Link-Label IHC Detection Systems; Bio-Genex, San Ramon, CA), visualized with Vector Red Substrate (SK-5100; Vector Laboratories, Burlingame, CA), and counterstained with hematoxylin. Negative control slides were performed without primary antibody. Control slides known to be positive for each antibody were incorporated. The total number of epithelial cells was enumerated in all glands and processed using Image-Pro Plus 5.1 software (Media Cybernetics,

Bethesda, MD). Ki-67 and caspase 3 staining was quantified by counting the number of positively stained nuclei among 100 cells on grids in three randomly chosen fields from different sections.

Cell Proliferation Assay

Cell proliferation was measured with the use of a CellTiter 96 AQueous Non-Radioactive Cell Proliferation Assay (Promega). Briefly, prostate cancer cells were plated in 96-well plates at a density of 2×10^3 per well in 100 µl of medium. After attachment, cells were treated with decorin or biglycan at varying concentrations and times and in the presence or absence of 2 µM AG1478 or 0.5 µM bicalutamide. After treatment, 20 µl of combined 3-(4,5-dimethylthiazol-2-yl)-5-(3-carboxymethoxyphenyl)-2-(4-sulfophenyl)-2*H* tetrazolium, inner salt (MTS)/phenazine methosulfate solution was then added and incubated for 2 hours at 37°C. The absorbance of each well at 490 nm was measured using an ELISA plate reader. Data represent the average absorbance of three wells, and error bars represent SDs.

DNA Synthesis

Cells were plated in 24-well plates at density of 2×10^3 per well. After 24 hours, culture media were supplemented with 5 µCi/ml [^{3}H]-thymidine, and cells were incubated with decorin or biglycan (0.4, 1, and 2 µM) for 24 hours. Cells were then washed with balanced salt solution (BSS) and trypsinized (200 µl of 0.05% trypsin for 5 minutes), then 400 µl of BSS was added. Wells were rinsed with 400 µl of BSS and pooled with trypsin fluids. One milliliter of ice-cold 10% trichloroacetic acid and 50 µl of serum were added, and samples were vortexed then held on ice for 1 hour and centrifuged at 2000 rpm for 10 minutes at 4°C. Supernatants were removed, and pellets were washed five times with 2 ml of ice-cold 5% trichloroacetic acid. Pellets were dissolved in 500 µl of 0.5N NaOH. [^{3}H]-Thymidine incorporation was determined by liquid scintillation counting.

Cytosolic and Nuclear Protein Extracts from LNCaP Cells

LNCaP cells were seeded in 100-mm dishes at a density of 2×10^6 cells per dish. After attachment, cells were treated with decorin (2 µM) or biglycan (2 µM) for 24 hours. Cells were then washed three times with ice-cold PBS and rinsed with 1× hypotonic buffer containing 20 mM HEPES (pH 7.9), 1 mM EDTA, 1 mM EGTA, 1 mM DL-dithiothreitol, and 0.5 mM phenylmethyl sulfonyl fluoride (PMSF). Cells were lysed with 200 µl of 1× hypotonic buffer containing 0.2% NP-40. Cell lysates were centrifuged for 20 seconds at 15,000 rpm at 4°C. Supernatants (cytosolic extracts) were transferred to a new tube and kept at –20°C. The pellet was resuspended in 50 µl of 1× high salt buffer (420 mM NaCl, 20 mM HEPES, pH 7.9, 1 mM EDTA, 1 mM EGTA, 20% glycerol, 1 mM DL-dithiothreitol, 0.5 mM PMSF) and incubated on ice for 30 minutes. After centrifugation at 12,000 rpm for 20 minutes at 4°C, the supernatant was harvested as the nuclear protein extract and stored at –80°C. Protein concentration was determined with a Lowry protein assay. Western blot assay was performed using antibodies recognizing the cytosolic protein, glyceraldehyde-3-phosphate dehydrogenase, or the nuclear protein, cyclic adenosine monophosphate response element binding protein.

Western Blot Assay

Prostate tissues were homogenized and cells were lysed in ice-cold lysis buffer (25 mM Tris-HCl, 150 mM NaCl, 1% Triton X-100, and 0.1 mg/ml PMSF) with 1× proteinase and 1× phosphatase inhibitors (Roche Applied Science, Indianapolis, IN). For the analysis of decorin core protein, lysis solution was dialyzed against 100 mM Tris, 30 mM sodium acetate, pH 8.0 for 24 hours at 4°C, and then digested by chondroitinase ABC at 37°C overnight. Protein extracts were electrophoresed by 12.5% SDS-PAGE and transferred to a nitro-cellulose membrane. After blocking with 5% nonfat dry milk, the membrane was washed three times with TBS/Tween-20 and incubated with the primary antibody diluted in 3% BSA at 4°C overnight. The blot was washed in TBS/Tween-20 and incubated for 1 hour with a horseradish peroxidase–conjugated secondary antibody diluted at 1:2000 for goat antimouse and goat antirabbit. The signal was detected using the chemiluminescent detection system (Pierce, Rockford, IL).

Immunofluorescence Analysis for AR

LNCaP cells were plated on coverslips in wells of a 24-well plate containing RPMI-1640 medium with 10% FBS. Cells were treated with 2 µM decorin or 2 µM biglycan for 24 hours followed by incubation with and without 1 nM DHT for 2 hours. Cells were then fixed with 10% formalin for 30 minutes. Coverslips were rinsed with PBS and permeabilized with 0.2% Triton X-100 for 30 minutes, then washed three times with PBS and incubated with anti-AR antibody (1:100; Santa Cruz Biotechnology) for 1 hour. After washing with PBS, cells were incubated with Alexa Fluor 488 goat antirabbit immunoglobulin G (Invitrogen) for 1 hour along with 4′,-6-diamidino-2-phenylindole (30 nM) for 15 minutes in the dark and washed three times with PBS. Cell images were captured under microscope with a digital camera and processed using Image-Pro Plus 5.1 software.

EGFR Gene Silencing by Small Interfering RNA

Two small interfering RNA (siRNA) specific for human *EGFR* gene was purchased from Qiagen (Hs_EGFR_10 HP Validated siRNA, Cat. No. SI02660140 and Hs_EGFR_12 HP Validated siRNA, Cat. No. SI02663983; Germantown, MD). For knockdown of EGFR in LNCaP cells, the individual siRNA was tested for EGFR and phospho-EGFR knockdown by Western blot assay. The most effective single siRNA (SI02663983) was used for further experiments. LNCaP cells were plated in a six-well plate at 2.0×10^5 cells and were transfected with siRNA and Lipofectamine 2000 (Invitrogen) according to the manufacturer's protocol. Control cells were transfected with a negative control siRNA. At 6 hours after transfection, each well was supplemented with growth medium containing 1% FBS for 24 hours. Cells were treated with decorin (2 µM) for 48 hours followed by EGF (100 ng/ml) for 15 minutes and were harvested to measure the amount of AR and AR phosphorylation.

Caspase 3 Activity Measurement

PC3 and LNCaP cells (10^3 cells per well) were cultured in 96-well plates for 24 hours then treated for 48 hours with decorin (2 µM) in the presence or absence of pretreatment with AG1478 (2 µM, 30 minutes), bicalutamide (0.5 µM for 90 minutes), or a combination of both. Caspase 3 activity was measured with the Caspase–Glo 3/7 Assay in which 30 µl of Caspase–Glo 3/7 reagent was added to each well and incubated for 1 hour at room temperature. Luminescence was measured with a Reporter Microplate luminometer (Turner BioSystems, Sunnyvale, CA).

Statistical Analysis

Data are expressed as the mean ± SD. Statistical analysis was performed using one-way analysis of variance. *P* values <.05 were considered statistically significant.

Results

Endogenous Decorin Expression Was Reduced, and an Exogenous Recombinant Decorin Inhibits Prostate Cancer Growth

Conditional deletion of the *Pten* gene in mouse prostate epithelium results in hyperplasia at 4 weeks of age and progression through carcinoma *in situ* to invasive adenocarcinoma by 16 weeks [34]. We have observed that endogenous decorin core protein levels in Pten null prostate glands are markedly lower compared with glands from Pten$^{P+/+}$ mice (data not shown). To determine the effect of systemic delivery of decorin on prostate cancer development, 4-week-old male Pten$^{P-/-}$ mice were randomized into three treatment groups to receive alternate-day intraperitoneal injections of saline, human recombinant decorin, or human recombinant biglycan (a related small leucine-rich proteoglycan, as negative control). At 12 weeks, mice were necropsied, prostate glands were weighed, and pathologic changes were evaluated. Decorin treatment resulted in a significant decrease in tumor weight compared with control groups (Figure 1*A*). Pathologic evaluation confirmed that histologic progression of tumors was retarded in decorin-treated animals, which generally developed prostate lesions with intermediate histopathology, carcinoma *in situ*, whereas mice injected with saline had a higher percentage of invasive adenocarcinoma (Figure 1*B*). Furthermore, cell proliferation as measured by Ki-67 immunostaining was
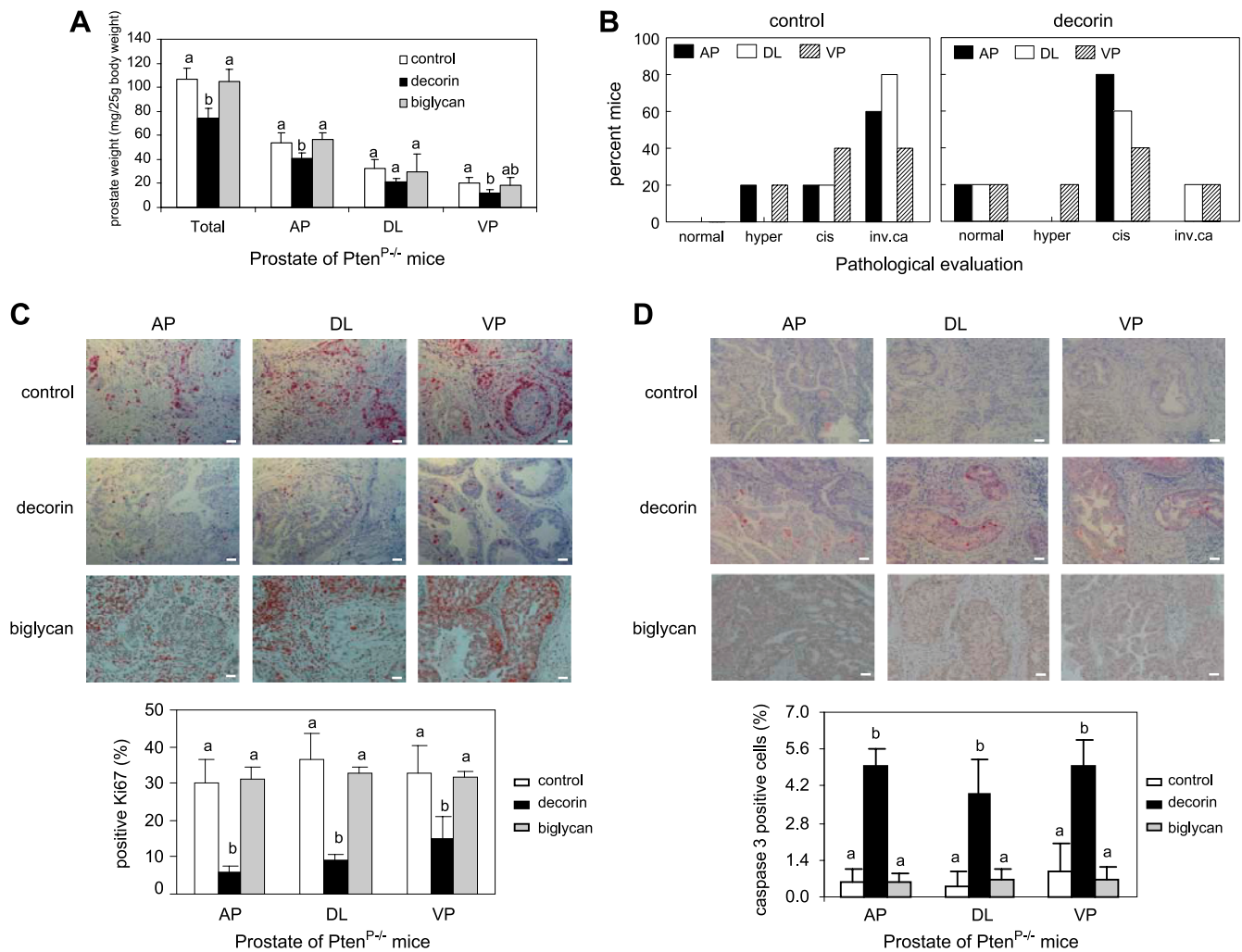

Figure 1. Exogenous decorin core protein inhibited the growth of prostate tumor in Pten$^{P-/-}$ mice. (A) Mice (*n* = 5 mice each group) were treated with decorin (10 mg/kg body weight), biglycan (10 mg/kg body weight), or saline through intraperitoneal injection for 12 weeks after weaning. The anterior (AP), dorsolateral (DL), and ventral (VP) prostate lobes were weighed and calculated as milligrams per 25-g body weight. Data were expressed as means ± SD and analyzed by one-way analysis of variance. Values with different letters are significantly different (*P* < .05). (B) Prostate grading of 10 Pten$^{P-/-}$ mice treated with either decorin (10 mg/kg body weight) or saline (control) was analyzed in AP, DL, and VP lobes using a double-blind method. When complex histologic diagnosis was found, the most advanced type was indicated. *cis* indicates carcinoma *in situ*; *hyper*, hyperplasia; *inv. ca*, invasive adenocarcinoma. (C) Pten$^{P-/-}$ mice treated with decorin (10 mg/kg body weight), biglycan (10 mg/kg body weight), or saline were randomly selected to analyze cell proliferation in prostate glands using immunohistochemistry with anti–Ki-67 antibody. Photos are representative of results obtained from three mice per group. Scale bar, 100 μm. Histograms at bottom show quantification of Ki-67–positive cells. (D) Pten$^{P-/-}$ mice treated with decorin (10 mg/kg body weight), biglycan (10 mg/kg body weight), or saline were randomly selected to measure apoptosis in prostate glands using immunohistochemistry with anti–cleaved caspase 3 antibodies. Photos are representative of results obtained from three mice per group. Scale bar, 100 μm. Histograms at the bottom show quantification of cleaved caspase 3–positive cells.
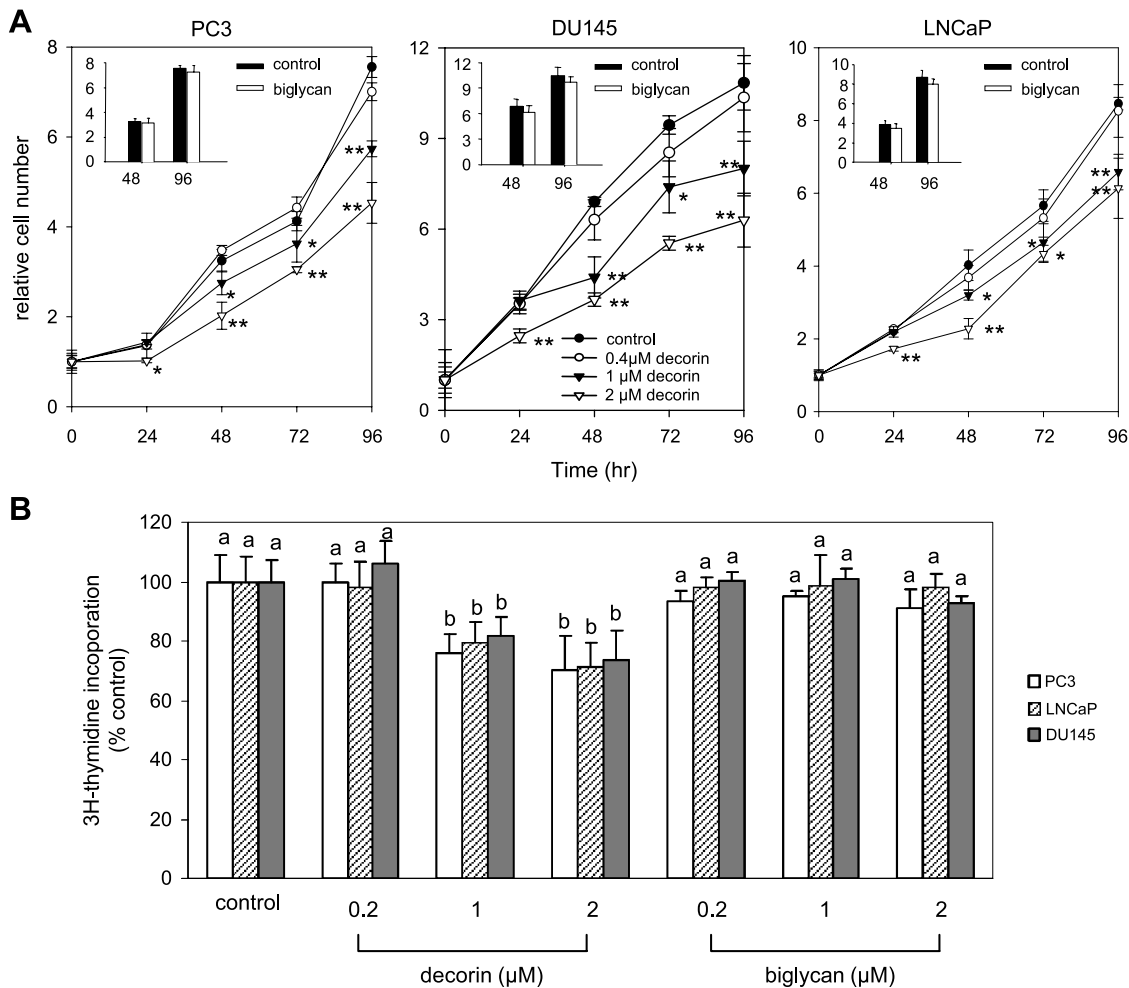
Figure 2. Decorin inhibited the growth of human prostate cancer cells. (A) PC3, DU145, and LNCaP cells were treated with decorin (0, 0.4, 1, and 2 μM) or biglycan (2 μM, insets), and cell number was measured as absorbance at 490 nm at the indicated times using MTS assay. Data are expressed as fold increases relative to pretreatment (0 time) for each treatment. *P < .05 or **P < .01, compared with control at the same observed time point. (B) PC3, DU145, and LNCaP cells were treated with decorin or biglycan at 0.2, 1, and 2 μM for 24 hours. DNA synthesis was measured by [^{3}H]-thymidine incorporation. Values shown are thymidine incorporation as a percent of control (no decorin) and represent mean $\pm$ SD (n = 3). Values with different letters are significantly different (P < .05).

dramatically reduced in all prostate lobes of decorin-treated animals (Figure 1C), and apoptosis as measured by cleaved caspase 3 immunostaining was significantly higher (Figure 1D). All of these measures were consistent in supporting a tumor-inhibitory role *in vivo* for systemically delivered decorin.

Decorin Inhibited the Growth of Human Prostate Cancer Cells

To test if decorin had a growth-inhibitory effect on human prostate cancer cells, androgen-independent (PC3 and DU145) and androgen-dependent (LNCaP) cell lines were treated with decorin. A significant decrease in proliferation of all three cell lines was observed in a dose-dependent manner after 1 to 4 days of treatment with decorin (Figure 2A). Decorin (1 and 2 μM) also inhibited DNA synthesis as measured by [^{3}H]-thymidine incorporation, within as little as 24 hours in PC3, LNCaP, and DU145 cells (Figure 2B). The effect was specific for decorin because biglycan had no significant effect on proliferation or DNA synthesis of the prostate cancer cells (Figure 2, A, insets, and B).

Decorin Downregulates EGFR

Transmission of extracellular signals often starts with binding of a growth factor to surface receptors. Previous studies have found that decorin is a ligand of EGFR that attenuates rather than triggers EGFR signaling in some epithelial-derived tumor cells [9,18,35]. Therefore, we measured EGFR expression by Western blot to determine the role of EGFR signaling in decorin-induced growth inhibition in prostate cancer. Figure 3A shows that systemic decorin treatment reduced total EGFR expression and rendered the phosphorylated EGFR undetectable in all prostate lobes of Pten$^{P-/-}$ mice. In human cell lines, our study showed that the basal level of EGFR expression was 1.6- and 1.3-fold higher in PC3 and DU145 cells, respectively, than in LNCaP cells (Figure 3B). Decorin decreased total EGFR after 5 to 10 minutes of exposure (Figure 3C), but the reduced total EGFR was subsequently returned to normal level (Figure 3B). Decorin dramatically reduced EGFR phosphorylation suggesting deactivation of EGFR (Figure 3, B and C). The dynamic effect of decorin on total EGFR *in vitro* (within the 48-hour exposure) indicates that a short exposure (<20 minutes) to decorin causes a reversible down-regulation of total EGFR, as was
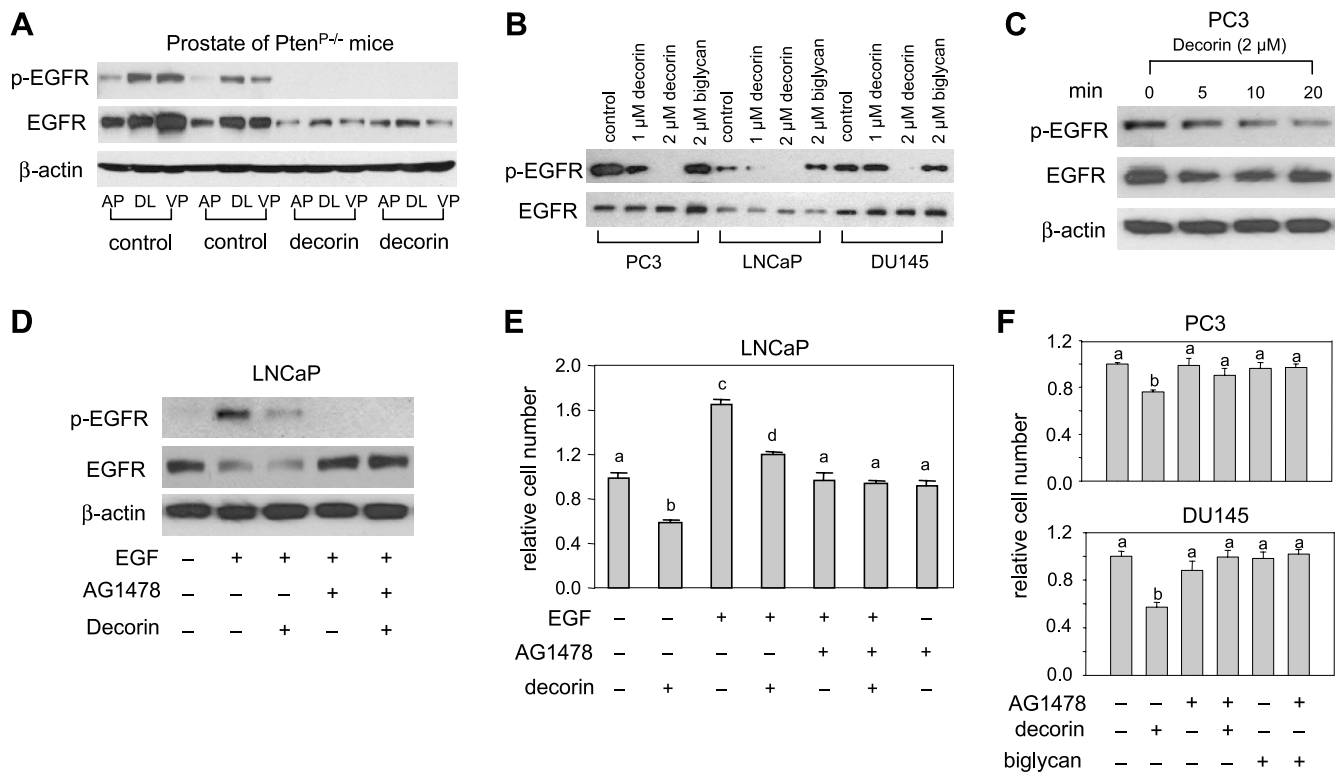
Figure 3. Decorin inhibited EGFR and EGFR phosphorylation in prostate of Pten$^{P-/-}$ mice and human prostate cancer cells. (A) Prostate tissues from AP, DL, and VP of Pten$^{P-/-}$ mice treated with decorin or saline ($n = 2$ mice each group) were homogenized with lysis buffer containing protease and phosphatase inhibitors. Protein extracts was analyzed by Western blots for EGFR, EGFR phosphorylation (Tyr 1068), and β-actin. (B) Cells were treated with decorin (1 and 2 μM) or biglycan (2 μM) for 48 hours. The cells were lysed, and EGFR and its phosphorylation (p-EGFR, Tyr 1068) were measured by Western blot analysis of 20-μg per well protein aliquots. Data shown are representative of three experiments with similar results. (C) PC3 cells were treated with decorin (2 μM) for 5, 10, or 20 minutes. Total proteins were used to measure EGFR and EGFR phosphorylation (Tyr 1068) by Western blot assay. Results are representative of two independent experiments. (D) LNCaP cells were treated with decorin (2 μM), AG1478 (2 μM), and/or EGF (100 ng/ml) for 10 minutes. Total proteins were analyzed by Western blot analysis with anti–phospho-EGFR (Tyr 1068) or anti–total EGFR antibodies. Results are representative of two independent experiments. (E) Cells were exposed to decorin (2 μM), biglycan (2 μM), AG1478 (2 μM), and/or EGF (100 ng/ml) for 48 hours. Cell number was measured by MTS. Values representing the mean ± SD ($n = 4$) with different letters indicate significant differences ($P < .05$). (F) PC3 and DU145 cells were exposed to EGFR kinase inhibitor, AG1478 (2 μM, pretreated for 30 minutes), decorin (2 μM), or biglycan (2 μM). Cell number was measured by MTS after 72 hours. Values representing the mean ± SD ($n = 4$) with different letters indicate significant differences ($P < .05$).

observed in A431 human squamous carcinoma cells [29]. It is possible that changes in the cellular composition of the tumor are reflected in our *in vivo* measures. At the very least, these data imply that decorin prevents EGFR phosphorylation *in vivo* as well as *in vitro*.

We also examined EGFR phosphorylation in response to EGF. LNCaP cells were treated with decorin and/or Tyrphostin AG1478 (specific inhibitor of the EGFR tyrosine kinase) and/or EGF for 10 minutes. EGF-induced EGFR phosphorylation (Figure 3D) and cell proliferation (Figure 3E) were attenuated by decorin or AG1478. EGF reduced total EGFR, and decorin did not block the effect (Figure 3D). In addition, AG1478 partially reversed the inhibitory effect of decorin on cell proliferation in LNCaP cells (Figure 3E) and totally reversed it in PC3 cells and DU145 cells (Figure 3F). An equal amount of recombinant human biglycan was essentially ineffective, indicating that the effects on EGFR phosphorylation and cell proliferation were specific to decorin (Figure 3, *B* and *F*).

Decorin Inhibits AR Expression and Nuclear Translocation

Androgen is known to modulate the development of human prostate cancer by binding to AR. In addition, AR and Pten coexpression is associated with the response to hormonal treatment in androgen-dependent prostate cancer [36] and androgen ablation therapy has been shown to prolong survival in Pten null mice [34]. We investigated the ability of decorin to regulate AR activity in prostate tissue of Pten$^{P-/-}$ mice and human prostate cancer cells. As shown by Western blot analysis in Figure 4A, decorin markedly inhibited the expression and phosphorylation of AR in all prostate lobes of Pten$^{P-/-}$ mice. In human prostate cancer cells, neither nonphosphorylated nor phosphorylated AR was detected in androgen-independent PC3 and DU145 lines, but in androgen-dependent LNCaP cells, decorin caused a dose-dependent inhibition of AR expression and phosphorylation, whereas biglycan was ineffective (Figure 4B). The expression of prostate-specific antigen (PSA) was similarly inhibited in LNCaP cells by decorin (Figure 4B). Immunofluorescent staining of LNCaP cells showed that the AR activating ligand, DHT, enhanced AR nuclear translocation and that this translocation was blocked by decorin (Figure 4C). This finding was supported by Western blot analysis of isolated nuclear and cytosolic fractions that showed markedly decreased AR in the nuclear fraction of cells treated with decorin (Figure 4D). Treatment of the cells with biglycan (2 μM) did not impact AR proteins

or AR translocation (Figure 4, *C* and *D*). To verify the effect of decorin on AR and AR phosphorylation, we used AR antagonist, bicalutamide. The inhibitory effects of decorin pretreatment on DHT-induced AR, AR phosphorylation, and PSA production in LNCaP cells were similar to that observed with bicalutamide pretreatment (Figure 4*E*). Moreover, they were mirrored by effects on cell proliferation (Figure 4*F*). Taken together, those results indicate that, in LNCaP cells, decorin down-regulates AR, inhibits AR nuclear translocation, depresses AR phosphorylation, and reduces the production of PSA.

Decorin Impacts the Cross Talking between EGFR and AR in LNCaP Cells

Previous studies showed that besides its classic location at the nucleus, the AR is a target at the plasma membrane for interactions with proteins involved in growth factor signaling [37]. We examined the interaction between EGFR and AR pathways that may be modified by decorin

in LNCaP cells. As shown in Figure 5*A*, EGF modestly increased AR expression and AR phosphorylation (*lane 1 vs lane 3*), and this effect was blocked by decorin (*lane 3 vs lane 4*). DHT also slightly activated EGFR phosphorylation, whereas decorin blocked the stimulatory effect of DHT (Figure 5*B*). This suggests that decorin may serve as a regulator of the interaction between EGFR and AR.

To further confirm the role for decorin in directional cross talk between EGFR and AR, LNCaP cells were treated with EGFR inhibitor, AG1478 or/and AR antagonist, bicalutamide, and then incubated with decorin for 48 hours. Figure 5*C* shows that, although AG1478 alone failed to reduce on AR expression or phosphorylation (*lanes 1* and *3*), it did partially reverse the inhibitory effects of decorin on AR (*lanes 2* and *4*). Similarly, bicalutamide alone had little ability to reduce EGFR phosphorylation (*lanes 1* and *5*) but partially reversed the inhibitory effect of decorin on EGFR (*lanes 2* and *6*). Thus, AG1478 and bicalutamide pretreatment modestly reduced the respective effects of
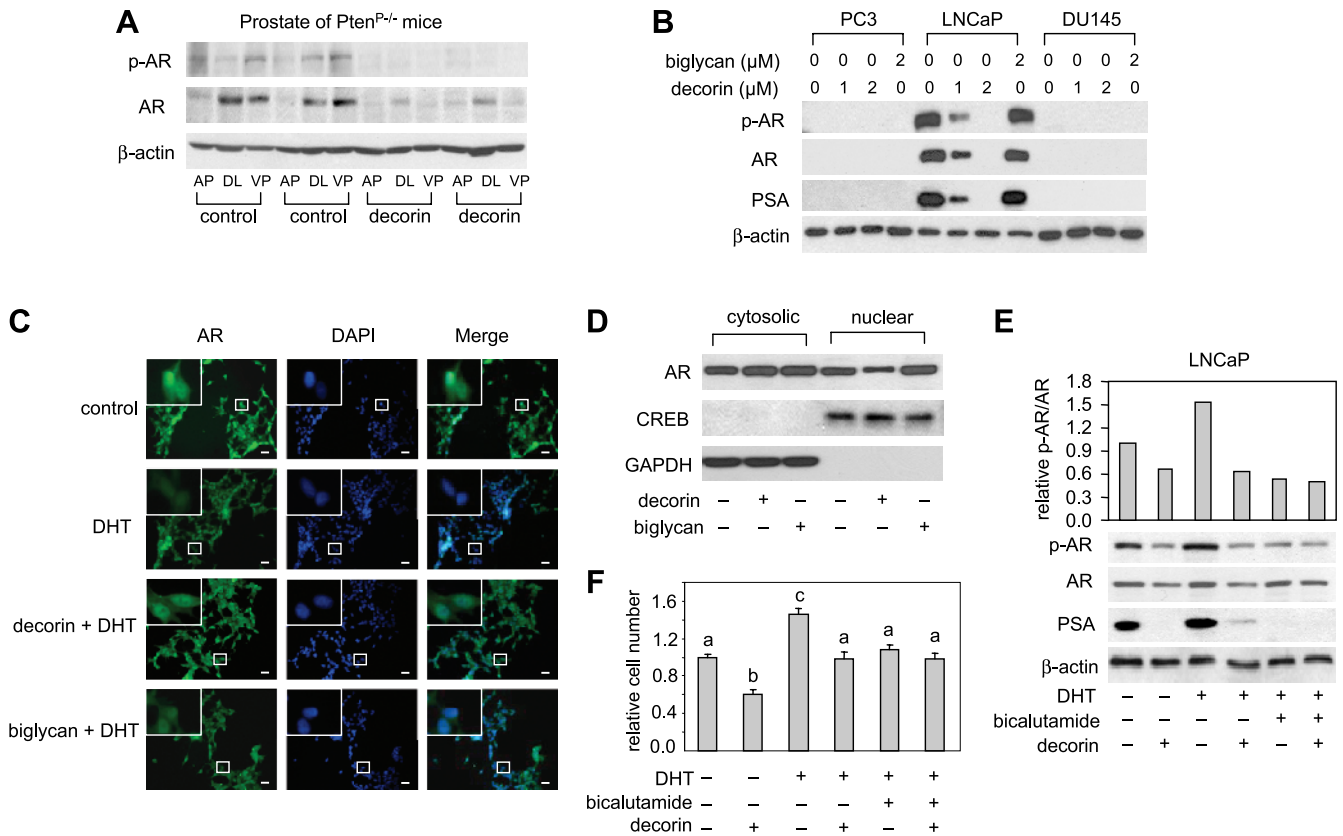

Figure 4. Decorin inhibited AR and production of PSA in prostate of Pten$^{P-/-}$ mice and LNCaP cells. (A) Protein extracts from prostate of Pten$^{P-/-}$ mice treated with decorin or saline (two mice in each group randomly selected) was used for Western blot analysis of AR, AR phosphorylation, and β-actin. (B) PC3, LNCaP, and DU145 cells were treated with decorin (1 and 2 μM) or biglycan (2 μM) for 48 hours. AR, AR phosphorylation (p-AR), and PSA proteins were measured by Western blots. Data shown are representative of two experiments with similar results. (C) LNCaP cells were seeded on coverslips in 24-well plates at the density of 5 × 10⁴ cells per milliliter and treated with decorin (2 μM) or biglycan (2 μM) for 24 hours followed by 1 nM DHT for 2 hours. Cells were then incubated with anti-AR antibody and visualized by Alexa Fluor 488 goat antirabbit immunoglobulin G and 4',6-diamidino-2-phenylindole staining. Representative photos of LNCaP cells were treated as indicated. Scale bar, 100 μm. Insets: High-magnification images of the areas in the white rectangles. Data shown are representative of two experiments. (D) LNCaP cells were exposed to decorin (2 μM) or biglycan (2 μM) for 24 hours. Cytosolic and nuclear proteins were extracted and AR was measured by Western blot analysis. Data shown are representative of three independent experiments. (E) LNCaP cells were treated with decorin and bicalutamide (0.5 μM, pretreated for 90 minutes) for 48 hours followed by DHT (1 nM) for 2 hours, and total proteins were isolated. AR, p-AR, and PSA were measured by Western blot assay. Data shown are representative of two independent experiments. (F) The growth of LNCaP cells was measured by MTS assay after treatment with DHT (1 nM), bicalutamide (0.5 μM), and decorin (2 μM) for 48 hours. Values representing the mean ± SD (n = 3) with different letters are significantly different (P < .05).
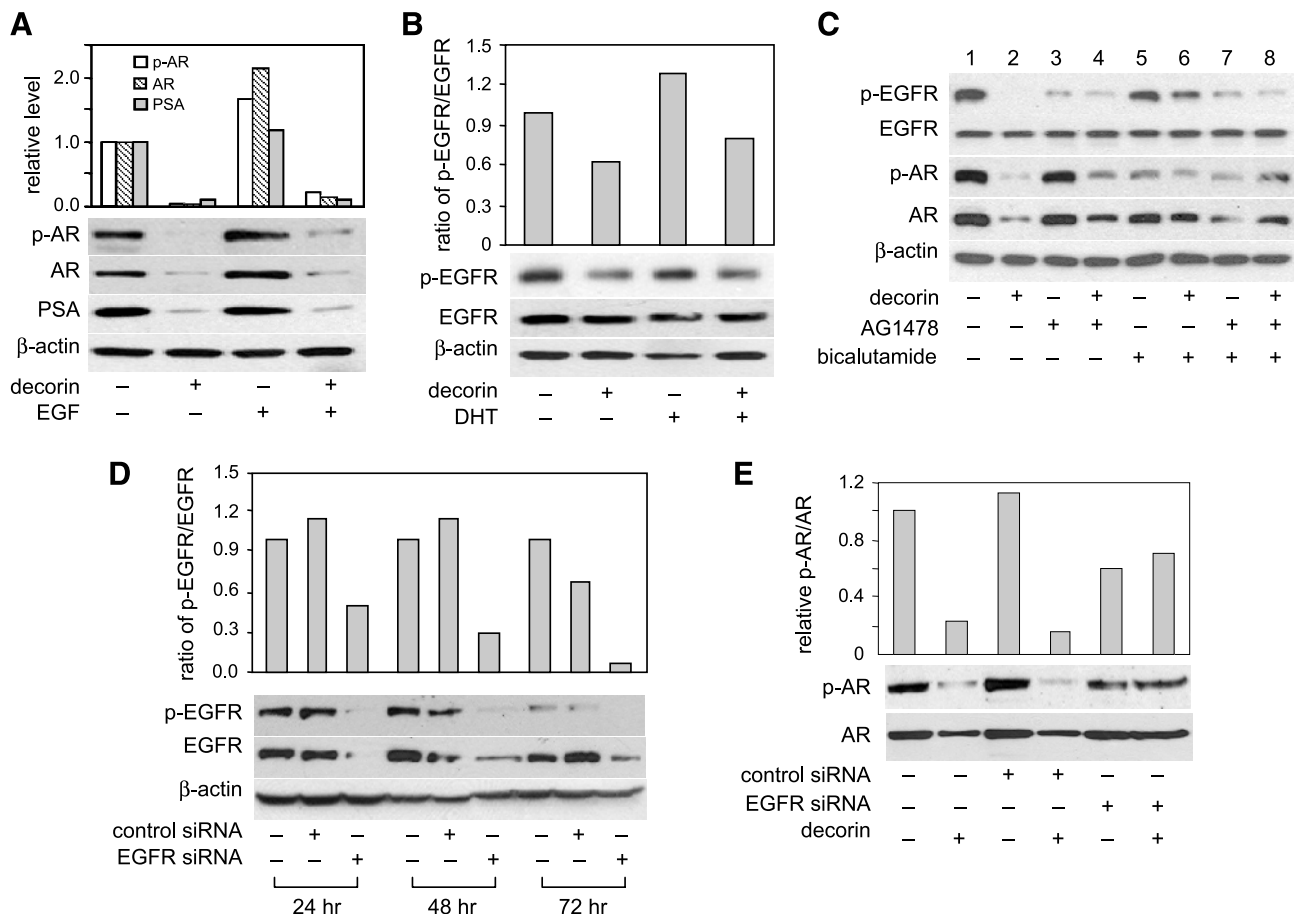
Figure 5. Decorin impacted the cross talk between EGFR and AR in LNCaP cells. (A) LNCaP cells were treated with decorin (2 μM) for 48 hours followed by EGF (100 ng/ml) for 15 minutes. Total protein (20 μg/lane) was used for Western blot analysis of AR, p-AR, and PSA. (B) LNCaP cells were exposed to decorin (2 μM) for 48 hours followed by DHT (1 nM) for 2 hours. Total protein was used for measurement of EGFR and p-EGFR (Tyr 1068). (C) LNCaP cells were treated with decorin (2 μM) or AG1478 (2 μM, pretreated for 30 minutes) or bicalutamide (0.5 μM, pretreated for 90 minutes) for 48 hours. AR, p-AR, PSA, EGFR, and p-EGFR (Tyr 1068) were measured by Western blot assay. (D) LNCaP cells were transfected with control siRNA or EGFR siRNA for 6 hours, then supplemented with growth medium containing 1% FBS for 24 hours. Cells were incubated with EGF (100 ng/ml) for 15 minutes before harvest. EGFR and p-EGFR (Tyr 1068) were measured by Western blot assay. (E) Cells were transfected with control siRNA or EGFR siRNA for 24 hours, then treated with decorin (2 μM) for 48 hours. AR and p-AR were measured as described before. All data shown are representative of two independent experiments.

decorin on EGFR and AR. Finally, LNCaP cells transfected with EGFR siRNA showed a large decrease in EGFR expression and phosphorylation by 24 hours (Figure 5D). This knockdown blocked the inhibitory effect of decorin on AR and AR phosphorylation (Figure 5E). Taken together, those results demonstrate that decorin suppresses the signaling pathway from EGFR to AR.

Decorin Inhibits PI3K/Akt Phosphorylation through Suppressions of EGFR and AR

The PI3K/Akt pathway is recognized as playing a critical regulatory role in the cell survival/death decision [38]. To determine the involvement of this pathway in the downstream signaling related to the suppression of EGFR and AR by decorin, we measured Akt and PI3K expression in cells treated with decorin. In PC3 cells, decorin inhibited Akt phosphorylation in a dose-dependent manner (Figure 6A). In these cells, EGF stimulated Akt phosphorylation (Figure 6B, *lanes 1* and *3*), an effect that was also reduced by decorin (*lanes 3* and *4*) or AG1478 (*lanes 3* and *5*). In LNCaP cells, decorin decreased Akt phosphorylation (Figure 6, *C* and *D*) and PI3K (Figure 6E). The inhibitory effects of

decorin pretreatment on DHT-induced Akt phosphorylation in LNCaP cells were similar to that observed with bicalutamide (Figure 6D). AG1478 or bicalutamide alone partially decreased the inhibitory effect of decorin on Akt phosphorylation and PI3K but, together, almost completely blocked the effects of decorin (Figure 6, *C* and *E*). Furthermore, the PI3K-specific inhibitor, wortmannin, also blocked the ability of decorin to inhibit phosphorylation of Akt (Figure 6F). These results together indicate that decorin inhibition of PI3K/Akt depends on the suppression of EGFR and AR.

Decorin Induces Apoptosis through Inhibition of EGFR and AR

To determine whether the observed inhibition of prostate cancer cell growth by decorin was due in part to apoptosis induction, we measured two biomarkers for apoptosis: caspase 3 activity and cleaved poly (ADP-ribose) polymerase (PARP) in PC3 cells and LNCaP cells. Decorin increased caspase 3 activity in both cell lines (Figure 7, *A* and *B*). In PC3 cells, EGF decreased caspase 3 activity, an effect that was blocked by decorin and by AG1478 (Figure 7A). In LNCaP cells, DHT reduced caspase 3 activity, an effect that was attenuated by treatment with decorin
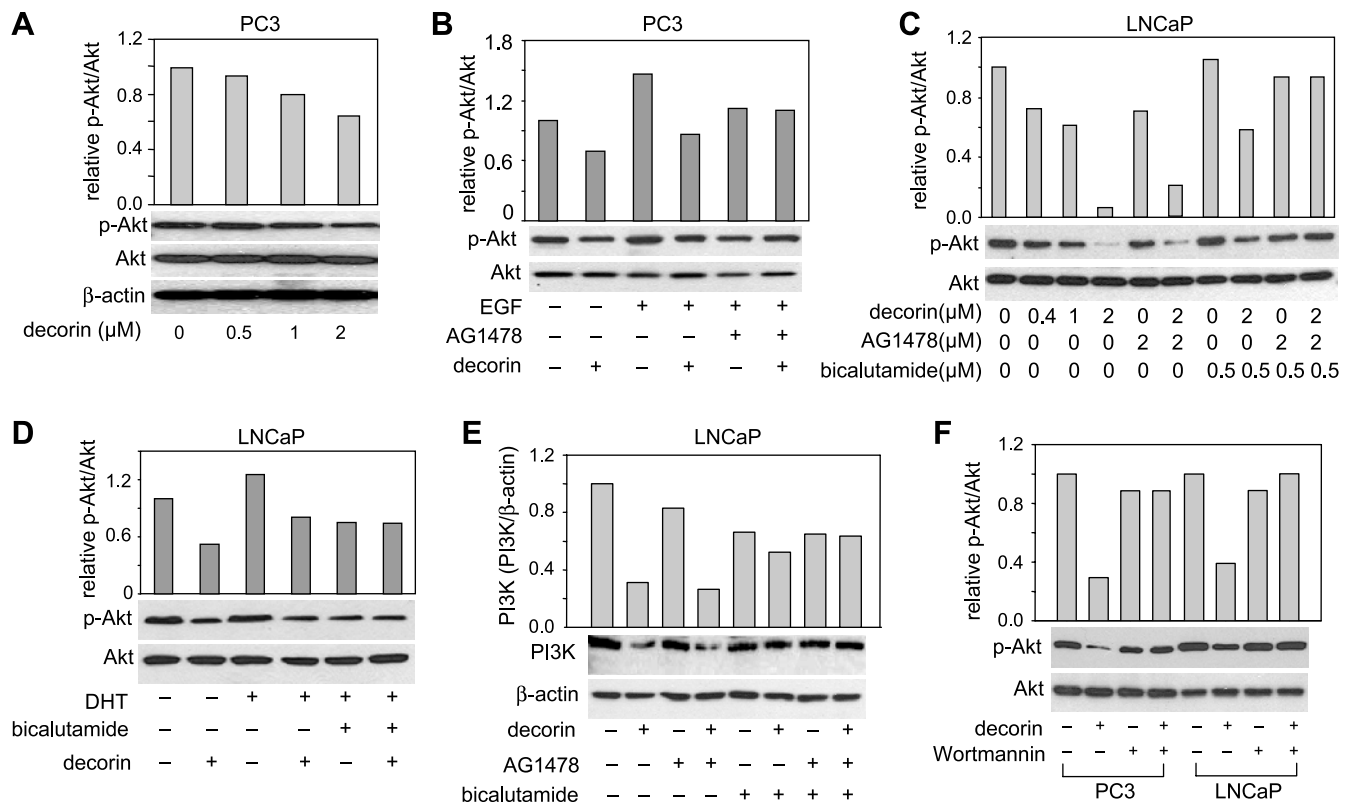
Figure 6. Decorin inhibited PI3K/Akt pathway through EGFR/AR in PC3 and LNCaP cells. (A) PC3 cells were treated with decorin for 48 hours. Protein extracts were used for Western blot analysis of total Akt and Akt phosphorylation (p-Akt, Ser 473). (B) PC3 cells were treated with decorin (2 μM) or AG1478 (2 μM, pretreated for 30 minutes) either alone or together for 48 hours followed by EGF (100 ng/ml) for 15 minutes. Total protein was used to measure total Akt and p-Akt. (C) LNCaP cells were incubated with decorin (0.4, 1, and 2 μM), AG1478 (2 μM, pretreated for 30 minutes), or bicalutamide (0.5 μM, pretreated for 90 minutes) either alone or together for 48 hours. Total protein was used for Western blot analysis of total Akt and p-Akt. (D) LNCaP cells were exposed to decorin and bicalutamide (0.5 μM, pretreated for 90 minutes) for 48 hours followed by 1 nM DHT for 2 hours. Total protein was used for Western blot analysis of total Akt and p-Akt. (E) LNCaP cells were treated with decorin (2 μM), AG1478 (2 μM, pretreated for 30 minutes), or bicalutamide (0.5 μM, pretreated for 90 minutes) either alone or together for 24 hours. The cells were lysed, and PI3K was measured by Western blot assay. (F) PC3 and LNCaP cells were pretreated with PI3K inhibitor, wortmannin (50 nM), for 30 minutes followed by decorin (2 μM) treatment of 48 hours. Total Akt and p-Akt were measured by Western blot assay. All data shown are representative of two independent experiments.

as well as bicalutamide (Figure 7B). The effects of decorin on apoptosis were confirmed in Western blot assays of PARP cleavage (Figure 7, C and D). Decorin increased cleaved PARP in PC3 and LNCaP cells. Decorin-induced PARP cleavage was markedly reduced by the EGFR inhibitor AG1478 in PC3 cells but only partially reduced by this agent in LNCaP cells. The AR antagonist, bicalutamide, also decreased decorin-induced PARP cleavage in LNCaP cells, and the combination of AG1478 and bicalutamide completely blocked decorin-induced PARP cleavage in these cells. These findings suggest that decorin induces apoptosis through the inhibition of EGFR and AR signaling in prostate cancer cells.

Discussion

Androgen-independent progression of prostate cancer does not seem to involve AR loss but instead results from inappropriate activation of AR [39,40]. This suggests that AR signaling may continue to play a critical role in the development and progression of prostate cancer. In addition, prostate cancer cells commonly overexpress several growth factors and their cognate receptors, including EGFR [1,41]. Enhanced EGFR expression is reported to be associated with high grades of prostate cancer malignancies [42]. More importantly, distinct oncogenic

products are activated through the stimulation of AR or EGFR, and interaction between growth factor signal transduction pathways and AR signaling propels the proliferation, survival, and invasion of prostate tumor cells, that is, through disease progression [1]. Therefore, the integration of external signals through the modulation of EGFR and AR activities could lead to a promising strategy for therapy in prostate cancer. Here, we have demonstrated that systemic delivery of decorin inhibits the progression of prostate cancer in Pten$^{P-/-}$ mice by inhibition of proliferation and stimulation of apoptosis. Similar effects were observed *in vitro* using human prostate cancer cell lines treated with exogenous decorin. Our study has further shown that exogenous decorin not only suppresses EGFR and AR expression and phosphorylation but also impacts their cross talk. This resulted in the inhibition of PI3K and Akt phosphorylation followed by an induction of apoptosis. These findings emphasize the potentially cooperative effect of simultaneous blockade of EGFR and AR signaling, such as that achieved by decorin, in the inhibition of prostate tumor growth.

An analysis of changing expression patterns of EGF and the EGFR during prostate cancer progression indicates that a switch from paracrine to autocrine EGF signaling is important to the autonomous growth of androgen-independent cells [43]. Recent studies with human lung, liver,

colorectal, and cervical tumor cells have found that decorin can directly interact with EGFR to regulate tumor cell growth [26,29]. Our data show that the basal levels of EGFR per milligram of cell protein are higher in androgen-independent PC3 and DU145 cells than in androgen-dependent LNCaP cells. Meanwhile, AR expression was not detectable in PC3 and DU145 cells. Exogenous decorin inhibited the growth of human prostate cancer cells by suppressing EGFR phosphorylation and its downstream signaling, PI3K/Akt, and by triggering apoptosis. Thus, decorin was a powerful regulator of androgen-independent prostate cancer cell growth. In addition to EGFR, previous studies have shown that decorin can also interact with other tyrosine kinase receptors such as insulin-like growth factor 1 receptor [44,45], vascular endothelial growth factor receptor [46], and Met receptor [47]. Those receptors play important roles in tumor progression and are now being regarded as targets for cancer therapy [48]. Further studies are required to clarify a role for these receptors in the inhibitory effect of decorin in prostate cancer.

AR classically acts at the nuclear level; however, it may also be located at the plasma membrane, where its interacts with proteins involved in growth factor signaling, such as Src kinase family members [49], caveolin 1 [50], and PI3K [51]. AR also modulates Akt activation through a PI3K-dependent mechanism [10,52]. PI3K/Akt activation was shown to promote the proliferation of diverse cancer cells including those of the prostate [38,53,54]. Our results show that in androgen-dependent LNCaP cells, decorin inhibited AR nuclear translocation, leading to decreased PSA expression and a suppressed PI3K/Akt signaling pathway. These inhibitory activities were partially reversed by the EGFR inhibitor, AG1478, and by the AR antagonist, bicalutamide, and completely abolished by the combination of bicalutamide and AG1478. Decorin also reduced DHT- or EGF-induced effects on AR and AR phosphorylation, whereas EGFR knockdown by siRNA abolished the inhibitory effect of decorin. These results suggest that decorin inhibits AR signaling to reduce the proliferation of androgen-dependent prostate cancer cells through a mechanism involving an interaction between AR and EGFR. Apparently, directional signaling from AR to EGFR was also impacted by decorin because the AR antagonist, bicalutamide, abrogated the effect of decorin on EGFR phosphorylation, which could be explained by the role of AR in the regulation of EGFR endocytotic trafficking [55]
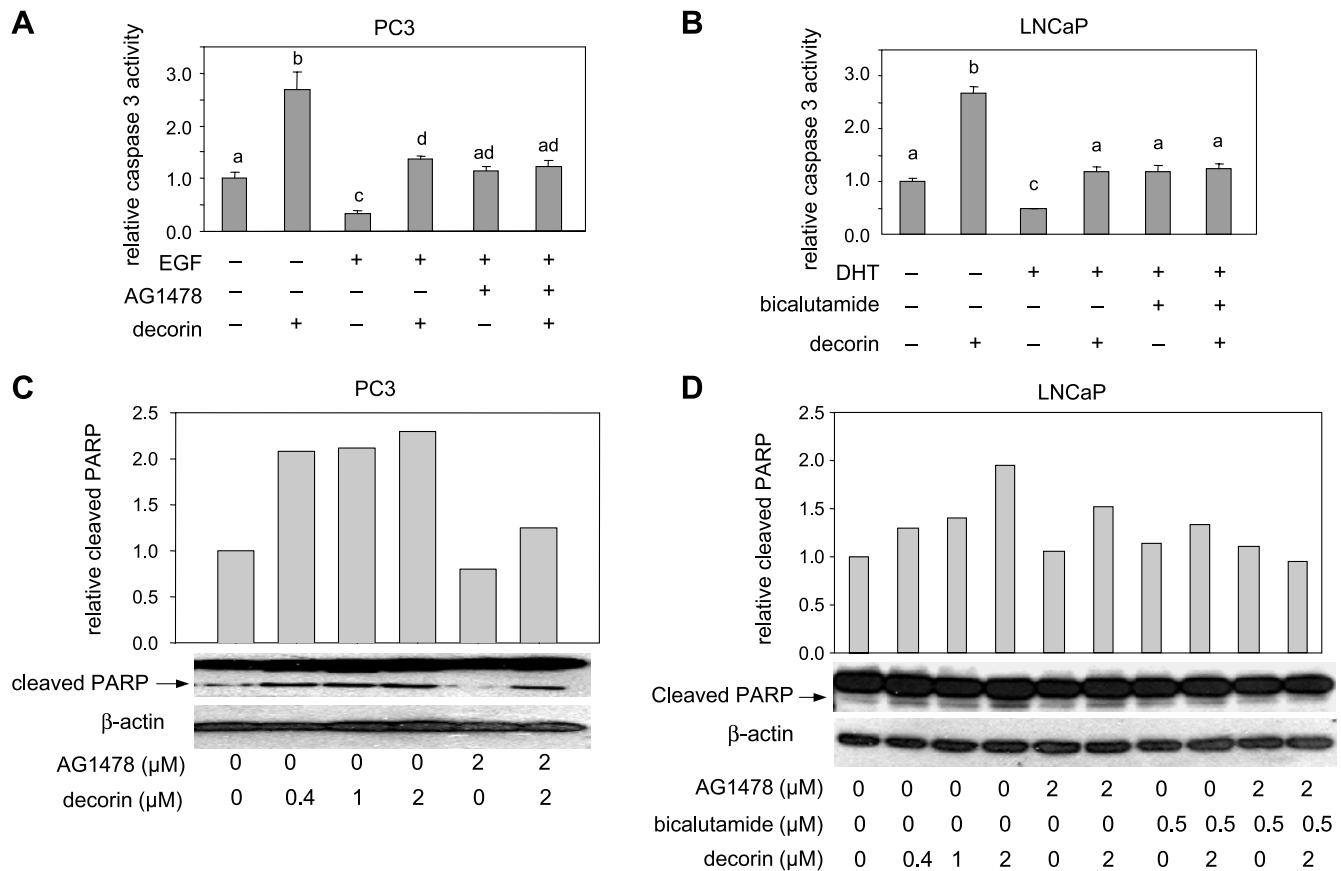

Figure 7. Decorin induced apoptosis by targeting EGFR and AR. (A) PC3 cells were treated with decorin (2 μM) or AG1478 (2 μM, pretreated for 30 minutes) followed by EGF (100 ng/ml) for 48 hours. Caspase 3 activity was measured with the Caspase–Glo 3/7 assay. Values representing the mean ± SD (n = 3) with different letters are significantly different (P < .05). (B) LNCaP cells were treated with decorin (2 μM) for 48 hours in the presence or absence of pretreatment with AG1478 (2 μM for 30 minutes), bicalutamide (0.5 μM for 90 minutes), or a combination of both. Caspase 3 activity was measured with the Caspase–Glo 3/7 assay. Values representing the mean ± SD (n = 3) with different letters are significantly different (P < .05). (C) PC3 cells were treated with decorin or the EGFR inhibitor, AG1478 (2 μM, pretreated for 30 minutes), for 48 hours, then cleaved PARP was measured by Western blot assay. Data shown are representative of two experiments with similar results. (D) LNCaP cells were treated with decorin for 72 hours in the presence or absence of pretreatment with AG1478 (2 μM for 30 minutes), bicalutamide (0.5 μM for 90 minutes), or a combination of both. Cleaved PARP was identified by Western analysis. Data shown (C and D) are representative of two independent experiments.
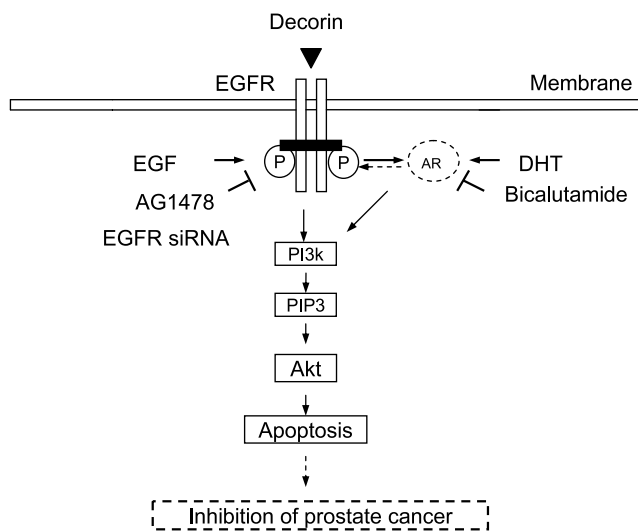
Figure 8. A schematic diagram illustrating signal transduction associated with the inhibitory effect of decorin on prostate tumor cell growth.

or EGFR/Erb2 heterodimer expression [56,57]. However, it remains to be determined whether decorin can directly or sequentially bind to and inhibit EGFR and AR or whether decorin acts indirectly to disrupt the EGFR and AR interaction and suppress downstream mediators including PI3K/Akt and apoptosis.

We observed that decorin inhibited the growth of androgen-dependent and androgen-independent prostate tumor cells by suppressing both EGFR- and AR-PI3K-Akt signaling. As shown in Figure 8, in AR-negative PC3 and DU145 cells, the effects of decorin seemed to be mediated entirely by the EGFR pathway, whereas the AR pathway provided an additional target in AR-positive LNCaP cells. Because of the central role of AR and EGFR in prostate cancer, new strategies and drugs to abrogate their signaling may have important clinical benefits. Our study provides a biologic basis for the inhibitory effect of endogenous and exogenous decorin on prostate tumor growth. Moreover, the clinical implications revealed by the mouse model suggest that decorin is a promising therapeutic agent for treating prostate cancer.

Acknowledgment

References

[1] Mimeault M and Batra SK (2006). Recent advances on multiple tumorigenic cascades involved in prostatic cancer progression and targeting therapies. *Carcinogenesis* **27**, 1–22.

[2] Chung LW, Baseman A, Assikis V, and Zhau HE (2005). Molecular insights into prostate cancer progression: the missing link of tumor microenvironment. *J Urol* **173**, 10–20.

[3] Ferdous Z, Wei VM, Iozzo R, Hook M, and Grande-Allen KJ (2007). Decorin-transforming growth factor-interaction regulates matrix organization and mechanical characteristics of three-dimensional collagen matrices. *J Biol Chem* **282**, 35887–35898.

[4] Köninger J, Giese NA, Bartel M, di Mola FF, Berberat PO, di Sebastiano P, Giese T, Büchler MW, and Friess H (2006). The ECM proteoglycan decorin links desmoplasia and inflammation in chronic pancreatitis. *J Clin Pathol* **59**, 21–27.

[5] Järveläinen H, Puolakkainen P, Pakkanen S, Brown EL, Höök M, Iozzo RV, Sage EH, and Wight TN (2006). A role for decorin in cutaneous wound healing and angiogenesis. *Wound Repair Regen* **14**, 443–452.

[6] Iozzo RV (1997). The family of the small leucine-rich proteoglycans: key regulators of matrix assembly and cellular growth. *Crit Rev Biochem Mol Biol* **32**, 141–174.

[7] Goldoni S and Iozzo RV (2008). Tumor microenvironment: modulation by decorin and related molecules harboring leucine-rich tandem motifs. *Int J Cancer* **123**, 2473–2479.

[8] Iozzo RV (1998). Matrix proteoglycans: from molecular design to cellular function. *Annu Rev Biochem* **67**, 609–652.

[9] Moscatello DK, Santra M, Mann DM, McQuillan DJ, Wong AJ, and Iozzo RV (1998). Decorin suppresses tumor cell growth by activating the epidermal growth factor receptor. *J Clin Invest* **101**, 406–412.

[10] Asundi VK and Dreher KL (1992). Molecular characterization of vascular smooth muscle decorin: deduced core protein structure and regulation of gene expression. *Eur J Cell Biol* **59**, 314–321.

[11] Mauviel A, Santra M, Chen YQ, Uitto J, and Iozzo RV (1995). Transcriptional regulation of decorin gene expression. Induction by quiescence and repression by tumor necrosis factor-alpha. *J Biol Chem* **270**, 11692–11700.

[12] Iozzo RV and Cohen I (1993). Altered proteoglycan gene expression and the tumor stroma. *Experientia* **49**, 447–455.

[13] Santra M, Skorski T, Calabretta B, Lattime EC, and Iozzo RV (1995). *De novo* decorin gene expression suppresses the malignant phenotype in human colon cancer cells. *Proc Natl Acad Sci USA* **92**, 7016–7020.

[14] Santra M, Mann DM, Mercer EW, Skorski T, Calabretta B, and Iozzo RV (1997). Ectopic expression of decorin protein core causes a generalized growth suppression in neoplastic cells of various histogenetic origin and requires endogenous p21, an inhibitor of cyclin-dependent kinases. *J Clin Invest* **100**, 149–157.

[15] De Luca A, Santra M, Baldi A, Giordano A, and Iozzo RV (1996). Decorin-induced growth suppression is associated with up-regulation of p21, an inhibitor of cyclin-dependent kinases. *J Biol Chem* **271**, 18961–18965.

[16] Csordás G, Santra M, Reed CC, Eichstetter I, McQuillan DJ, Gross D, Nugent MA, Hajnóczky G, and Iozzo RV (2000). Sustained down-regulation of the epidermal growth factor receptor by decorin. A mechanism for controlling tumor growth *in vivo*. *J Biol Chem* **275**, 32879–32887.

[17] Xaus J, Comalada M, Cardo M, Valledor AF, and Celada A (2001). Decorin inhibits macrophage colony-stimulating factor proliferation of macrophages and enhances cell survival through induction of p27(Kip1) and p21(Waf1). *Blood* **98**, 2124–2133.

[18] Iozzo RV, Moscatello DK, McQuillan DJ, and Eichstetter I (1999). Decorin is a biological ligand for the epidermal growth factor receptor. *J Biol Chem* **274**, 4489–4492.

[19] Yamaguchi Y, Mann DM, and Ruoslahti E (1990). Negative regulation of transforming growth factor-β by the proteoglycan decorin. *Nature* **346**, 281–284.

[20] Stander M, Naumann U, Dumitrescu L, Heneka M, Loschmann P, Gulbins E, Dichgans J, and Weller M (1998). Decorin gene transfer–mediated suppression of TGF-β synthesis abrogates experimental malignant glioma growth *in vivo*. *Gene Ther* **5**, 1187–1194.

[21] Grant DS, Yenisey C, Rose RW, Tootell M, Santra M, and Iozzo RV (2002). Decorin suppresses tumor cell–mediated angiogenesis. *Oncogene* **21**, 4765–4777.

[22] Fan H, Sulochana KN, Chong YS, and Ge R (2008). Decorin derived antiangiogenic peptide LRR5 inhibits endothelial cell migration by interfering with VEGF-stimulated NO release. *Int J Biochem Cell Biol* **40**, 2120–2128.

[23] Iozzo RV, Chakrani F, Perrotti D, McQuillan DJ, Skorski T, Calabretta B, and Eichstetter I (1999). Cooperative action of germ-line mutations in decorin and p53 accelerates lymphoma tumorigenesis. *Proc Natl Acad Sci USA* **96**, 3092–3097.

[24] Bi X, Tong C, Dockendorff A, Bancroft L, Gallagher L, Guzman G, Iozzo RV, Augenlicht LH, and Yang W (2008). Genetic deficiency of decorin causes intestinal tumor formation through disruption of intestinal cell maturation. *Carcinogenesis* **29**, 1435–1440.

[25] Reed CC, Gauldie J, and Iozzo RV (2002). Suppression of tumorigenicity by adenovirus-mediated gene transfer of decorin. *Oncogene* **21**, 3688–3695.

[26] Tralhão JG, Schaefer L, Micegova M, Evaristo C, Schönherr E, Kayal S, Veiga-Fernandes H, Danel C, Iozzo RV, Kresse H, et al. (2003). *In vivo* selective and distant killing of cancer cells using adenovirus-mediated decorin gene transfer. *FASEB J* **17**, 464–466.

[27] Biglari A, Bataille D, Naumann U, Weller M, Zirger J, Castro MG, and Lowenstein PR (2004). Effects of ectopic decorin in modulating intracranial glioma progression *in vivo*, in a rat syngeneic model. *Cancer Gene Ther* **11**, 721–732.

[28] Banerjee AG, Liu J, Yuan Y, Gopalakrishnan VK, Johansson SL, Dinda AK, Gupta NP, Trevino L, and Vishwanatha JK (2003). Expression of biomarkers modulating prostate cancer angiogenesis: differential expression of annexin II in prostate carcinomas from India and USA. *Mol Cancer* **2**, 34.

[29] Seidler DG, Goldoni S, Agnew C, Cardi C, Thakur ML, Owens RT, McQuillan DJ, and Iozzo RV (2006). Decorin protein core inhibits *in vivo* cancer growth and metabolism by hindering epidermal growth factor receptor function and triggering apoptosis via caspase-3 activation. *J Biol Chem* **281**, 26408–26418.

[30] Mercado ML, Amenta AR, Hagiwara H, Rafii MS, Lechner BE, Owens RT, McQuillan DJ, Froehner SC, and Fallon JR (2006). Biglycan regulates the expression and sarcolemmal localization of dystrobrevin, syntrophin, and nNOS. *FASEB J* **20**, 1724–1726.

[31] Berquin IM, Min Y, Wu R, Wu J, Perry D, Cline JM, Thomas MJ, Thornburg T, Kulik G, Smith A, et al. (2007). Modulation of prostate cancer genetic risk by omega-3 and omega-6 fatty acids. *J Clin Invest* **117**, 1866–1875.

[32] Lesche R, Groszer M, Gao J, Wang Y, Messing A, Sun H, Liu X, and Wu H (2002). Cre/loxP–mediated inactivation of the murine Pten tumor suppressor gene. *Genesis* **32**, 148–149.

[33] Wu X, Wu J, Huang J, Powell WC, Zhang J, Matusik RJ, Sangiorgi FO, Maxson RE, Sucov HM, and Roy-Burman P (2001). Generation of a prostate epithelial cell–specific Cre transgenic mouse model for tissue-specific gene ablation. *Mech Dev* **101**, 61–69.

[34] Wang S, Gao J, Lei Q, Rozengurt N, Pritchard C, Jiao J, Thomas GV, Li G, Roy-Burman P, Nelson PS, et al. (2003). Prostate-specific deletion of the murine Pten tumor suppressor gene leads to metastatic prostate cancer. *Cancer Cell* **4**, 209–221.

[35] Zhu JX, Goldoni S, Bix G, Owens RT, McQuillan DJ, Reed CC, and Iozzo RV (2005). Decorin evokes protracted internalization and degradation of the epidermal growth factor receptor via caveolar endocytosis. *J Biol Chem* **280**, 32468–32479.

[36] El Sheikh SS, Romanska HM, Abel P, Domin J, and Lalani el N (2008). Predictive value of PTEN and AR coexpression of sustained responsiveness to hormonal therapy in prostate cancer—a pilot study. *Neoplasia* **10**, 949–953.

[37] Bonaccorsi L, Muratori M, Carloni V, Zecchi S, Formigli L, Forti G, and Baldi E (2003). Androgen receptor and prostate cancer invasion. *Int J Androl* **26**, 21–25.

[38] Cantley LC (2002). The phosphoinositide 3-kinase pathway. *Science* **296**, 1655–1657.

[39] Chen CD, Welsbie DS, Tran C, Baek SH, Chen R, Vessella R, Rosenfeld MG, and Sawyers CL (2004). Molecular determinants of resistance to antiandrogen therapy. *Nat Med* **10**, 33–39.

[40] Chmelar R, Buchanan G, Need EF, Tilley W, and Greenberg NM (2007). Androgen receptor coregulators and their involvement in the development and progression of prostate cancer. *Int J Cancer* **120**, 719–733.

[41] Di Lorenzo G, Tortora G, D'Armiento FP, De Rosa G, Staibano S, Autorino R, D'Armiento M, De Laurentiis M, De Placido S, Catalano G, et al. (2002). Expression of epidermal growth factor receptor correlates with disease relapse and progression to androgen-independence in human prostate cancer. *Clin Cancer Res* **8**, 3438–3444.

[42] Harper ME, Glynne-Jones E, Goddard L, Mathews P, and Nicholson RI (1998).

[43] Scher HI, Sarkis A, Reuter V, Cohen D, Netto G, Petrylak D, Lianes P, Fuks Z, Mendelsohn J, and Cordon-Cardo C (1995). Changing pattern of expression of the epidermal growth factor receptor and transforming growth factor alpha in the progression of prostatic neoplasms. *Clin Cancer Res* **1**, 545–550.

[44] Schonherr E, Sunderkotter C, Iozzo RV, and Schaefer L (2005). Decorin, a novel player in the insulin-like growth factor system. *J Biol Chem* **280**, 15767–15772.

[45] Fiedler LR, Schonherr E, Waddington R, Niland S, Seidler DG, Aeschlimann D, and Eble JA (2008). Decorin regulates endothelial cell motility on collagen I through activation of insulin-like growth factor I receptor and modulation of $\alpha_2\beta_1$ integrin activity. *J Biol Chem* **283**, 17406–17415.

[46] Iacob D, Cai J, Tsonis M, Babwah A, Chakraborty C, Bhattacharjee RN, and Lala PK (2008). Decorin-mediated inhibition of proliferation and migration of the human trophoblast via different tyrosine kinase receptors. *Endocrinology* **149**, 6187–6197.

[47] Goldoni S, Humphries A, Nyström A, Sattar S, Owens RT, McQuillan DJ, Ireton K, and Iozzo RV (2009). Decorin is a novel antagonistic ligand of the Met receptor. *J Cell Biol* **185**, 743–754.

[48] Krause DS and Van Etten RA (2005). Tyrosine kinases as targets for cancer therapy. *N Engl J Med* **353**, 172–187.

[49] Migliaccio A, Castoria G, Di Domenico M, de Falco A, Bilancio A, Lombardi M, Barone MV, Ametrano D, Zannini MS, Abbondanza C, et al. (2000). Steroid-induced androgen receptor-oestradiol receptor β–Src complex triggers prostate cancer cell proliferation. *EMBO J* **19**, 5406–5417.

[50] Lu ML, Schneider MC, Zheng Y, Zhang X, and Richie JP (2001). Caveolin-1 interacts with androgen receptor. A positive modulator of androgen receptor mediated transactivation. *J Biol Chem* **276**, 13442–13451.

[51] Simoncini T, Hafezi-Moghadam A, Brazil DP, Ley K, Chin WW, and Liao JK (2000). Interaction of oestrogen receptor with the regulatory subunit of phosphatidylinositol-3-OH kinase. *Nature* **407**, 538–541.

[52] Baron S, Manin M, Beaudoin C, Leotoing L, Communal Y, Veyssiere G, and Morel G (2004). Androgen receptor mediates non-genomic activation of phosphatidylinositol 3-OH kinase in androgen-sensitive epithelial cells. *J Biol Chem* **279**, 14579–14586.

[53] Grille SJ, Bellacosa A, Upson J, Klein-Szanto AJ, van Roy F, Lee-Kwon W, Donowitz M, Tsichlis PN, and Larue L (2003). The protein kinase Akt induces epithelial mesenchymal transition and promotes enhanced motility and invasiveness of squamous cell carcinoma lines. *Cancer Res* **63**, 2172–2178.

[54] Majumder PK and Sellers WR (2005). Akt-regulated pathways in prostate cancer. *Oncogene* **24**, 7465–7474.

[55] Bonaccorsi L, Nosi D, Muratori M, Formigli L, Forti G, and Baldi E (2007). Altered endocytosis of epidermal growth factor receptor in androgen receptor positive prostate cancer cell lines. *J Mol Endocrinol* **38**, 51–66.

[56] Pignon JC, Koopmansch B, Nolens G, Delacroix L, Waltregny D, and Winkler R (2009). Androgen receptor controls EGFR and ERBB2 gene expression at different levels in prostate cancer cell lines. *Cancer Res* **69**, 2941–2949.

[57] Naderi A and Hughes-Davies L (2008). A functionally significant cross-talk between androgen receptor and ErbB2 pathways in estrogen receptor negative breast cancer. *Neoplasia* **10**, 542–548.

Expression of androgen receptor and growth factors in premalignant lesions of the prostate. *J Pathol* **186**, 169–177.